Low sensitivity of gross primary production to elevated CO_2 in a mature Eucalypt woodland

Authors: Jinyan Yang[1], Belinda E. Medlyn[1], Martin G. De Kauwe[2,3], Remko A. Duursma[1], Mingkai Jiang[1], Dushan Kumarathunge[1], Kristine Y. Crous[1], Teresa E. Gimeno[4,5], Agnieszka Wujeska-Klause[1], David S. Ellsworth[1]

Affiliation: [1] Hawkesbury Institute for the Environment, Western Sydney University, Penrith, NSW, Australia

[2] ARC Centre of Excellence for Climate Extremes, Sydney, NSW 2052, Australia

[3] Climate Change Research Centre, University of New South Wales, Sydney, NSW 2052, Australia

[4] Basque Centre for Climate Change, Scientific Campus of the University of the Basque Country, Leioa, Spain

[5] IKERBASQUE, Basque Foundation for Science, 48008, Bilbao, Spain

Correspondence to: Jinyan Yang (jinyan.yang@westernsydney.edu.au)

For submission to: Biogeosciences Discussions

No of words in abstract: 269

No of words in main text: 6705

No of Figures: 8

No of Tables: 1

Abstract

The response of mature forest ecosystems to rising atmospheric carbon dioxide concentration (C_a) is a major uncertainty in projecting the future trajectory of the Earth's climate. Although leaf-level net photosynthesis is typically stimulated by exposure to elevated C_a (eC_a), it is unclear how this stimulation translates into carbon cycle responses at whole-ecosystem scale. Here we estimate a key component of the carbon cycle, the gross primary productivity (GPP), of a mature native Eucalypt forest exposed to Free Air CO_2 Enrichment (the EucFACE experiment). In this experiment, light-saturated leaf photosynthesis increased by 19% in response to a 38% increase in C_a. We used the process-based forest canopy model, MAESPA, to upscale these leaf-level measurements of photosynthesis with canopy structure to estimate GPP and its response to eC_a. We assessed the direct impact of eC_a, as well as the indirect effect of photosynthetic acclimation to eC_a and variability among treatment plots via different model scenarios.

At the canopy scale, MAESPA estimated a GPP of 1574 g C m^{-2} yr^{-1} under ambient conditions across four years and a direct increase in GPP of +11% in response to eC_a. The smaller canopy-scale response simulated by the model, as compared to the leaf-level response, could be attributed to the prevalence of RuBP-regeneration limitation of leaf photosynthesis within the canopy. Photosynthetic acclimation reduced this estimated response to 10%. After taking in account the baseline variability in leaf area index across plots, we estimated a field GPP response to eC_a of 6% with a 95% confidence interval (-2, 14%). These findings highlight that the GPP response of mature forests to eC_a is likely to be considerably lower than the response of light-saturated leaf photosynthesis. Our results provide an important context for interpreting eC_a responses of other components of the ecosystem carbon cycle.

1. Introduction

Forests represent the largest long-term terrestrial carbon storage (Bonan, 2008; Pan et al., 2011). Atmospheric carbon dioxide concentration (C_a) has increased significantly since the beginning of the industrial era (Joos and Spahni, 2008), but the increase would have been considerably larger without forest carbon sequestration, which is estimated to have offset 25-33% of recent anthropogenic CO_2 emissions (Le Quéré et al. 2017). C_a is projected to continue to increase by 1-5 μmol mol^{-1} per year into the future (IPCC, 2014), but the rate of this rise depends on the magnitude of the forest feedback on C_a. At the leaf scale, the direct physiological effects of rising C_a are well understood: elevated C_a (eC_a) stimulates plant photosynthesis (Kimball et al. 1993; Ellsworth et al. 2012) and reduces stomatal conductance (Morison, 1985, Saxe et al. 1998), which together increase leaf water-use efficiency (De Kauwe et al. 2014). These physiological responses at the leaf scale can increase ecosystem carbon uptake, which in turn may result in increased carbon storage in the ecosystem, mitigating against the rise in C_a. However, projecting the response of the terrestrial carbon sink to future increases in C_a is a major uncertainty in models (Friedlingstein et al. 2014), highlighting an urgent need to make greater use of data from manipulative experiments at leaf scale to inform terrestrial biosphere models (Medlyn et al., 2015).

Our understanding of ecosystem responses to eC_a relies on both experiments and observations. However, results from different types of studies show some important areas of disagreement (Fatichi et al., 2019). At the global scale, satellite data provide evidence of a strong greening trend over the last 20 years, indicating an increase in leaf area and/or above-ground biomass, which has been attributed to the gradual increase in CO_2 (Donohue et al., 2009; Donohue et al., 2013; Yang et al., 2016; Zhu et al., 2016). A positive response of carbon uptake/greenness is also found in manipulative eC_a open-top chamber experiments with young trees (Eamus and Jarvis, 1989; Curtis and Wang 1998; Saxe et al. 1998; Medlyn et al., 1999) and ecosystem-scale FACE experiments in young, aggrading forest stands (Ainsworth and Long, 2005; Norby et al., 2005; , Ellsworth et al. 2012; Walker et al. 2019). In contrast, individual-tree experiments with mature trees (>30 years old) have found relatively small responses of tree growth to eC_a despite an apparent increase in leaf photosynthesis (Dawes et al., 2011; Sigurdsson et al., 2013; Klein et al., 2016). Also, tree-ring studies indicate an apparent lack of stimulation of vegetation growth in mature forests over the last century (Peñuelas et al. 2011; Silva and Anand, 2013; van der Sleen et al. 2014). These studies raise important questions about how mature ecosystems will respond to eC_a.

The Eucalyptus FACE experiment (EucFACE; Australia) is the first replicated, ecosystem-scale experiment where a mature native forest has been experimentally subjected to eC_a and provides a valuable case study to assess the response of a mature forest response to eC_a under field conditions (Ellsworth et al. 2017). Results from the first five years (2013-2018) of leaf gas exchange measurements showed a consistent stimulation of leaf-level light-saturated net photosynthesis (A) of 19% (Ellsworth et al., 2017; Wujeska-Klause et al., 2019). Nevertheless, the increase in A did not lead to a detectable change in above-ground growth (Ellsworth et al., 2017). These experimental results are consistent with empirical evidence arising from tree-ring studies (Peñuelas et al. 2011; Silva and Anand, 2013; van der Sleen et al. 2014) and also with experimental evidence from individual mature trees (Körner et al., 2005; Dawes et al., 2011; Klein et al., 2016).

As a first step towards reconciling the eC_a responses of leaf photosynthesis and above-ground growth in this experiment, here we quantify how the whole canopy carbon uptake, or gross primary productivity (GPP) was increased under eC_a. The response of GPP is important because it provides a reference point against which to compare the response of other components of ecosystem carbon balance, such as above-ground growth. It needs to be quantified explicitly because the response of GPP to eC_a may be quite different to that of leaf net photosynthesis. The leaf-level response of photosynthesis to eC_a is usually measured on sunlit leaves under saturating light (Ainsworth and Rogers, 2007). As a result, these leaf-level eC_a responses largely reflect the responses of the photosynthesis rate when limited by maximum Rubisco activity (V_{cmax}). However, depending on the canopy architecture and ambient light condition, the canopy could have many shaded leaves, which would mean that the emergent rate of photosynthesis could actually be limited by RuBP regeneration (J). RuBP-regeneration limited photosynthesis has a smaller response to eC_a than Rubisco-limited photosynthesis (Ainsworth and Rogers, 2007), resulting in a smaller response of GPP than leaf photosynthesis under saturating light.

The transition from RuBP-regeneration to Rubisco-limited photosynthesis of the canopy is determined by the ratio of the maximum capacities for RuBP-regeneration and Rubisco activity, J_{max} and V_{cmax} (Friend, 2001; Zaehle et al. 2014; Rogers et al., 2017). Wullschleger (1993) reported a J_{max}:V_{cmax} ratio of 2, which has been widely adopted in models (e.g., Wang et al., 1998; Luo et al., 2001; Rogers et al., 2017). However, recent studies have suggested the J_{max}:V_{cmax} ratio varies systematically across forest ecosystems and can range from 1 to 3 (Kattge and Knorr, 2007; Ellsworth et al., 2012; Kumarathunge et al., 2018). A lower J_{max}:V_{cmax} ratio results in more frequent RuBP-regeneration limitation of photosynthesis, which reduces the response of GPP to eC_a.

It is difficult to directly measure the eC_a effect on GPP. In some previous eC_a experiments, GPP has been estimated by scaling up from leaf-level measurements using a canopy model. Wang et al (1998) and Luo et al (2001) both used the tree array model, MAESPA, which can simulate the radiative transfer within and between tree crowns and can be parameterised to describe the spatial locations and sizes of trees in eC_a experiments. In these previous applications of MAESPA, the direct response of GPP to eC_a was consistently half of that observed at the leaf level because of a large contribution of RuBP-regeneration limited photosynthesis to GPP (Wang et al., 1998; Luo et al., 2001). However, the direct effect of eC_a on photosynthesis was modified by two major indirect effects. When LAI increased under eC_a, the additional leaf area amplified the GPP response by up to 60%. The other factor is the downregulation of photosynthesis under eC_a, or photosynthetic acclimation (Long et al., 2004; Ainsworth and Rogers, 2007; Rogers, et al., 2017). Under long-term exposure to eC_a, some plants have been observed to reduce nitrogen allocation to Rubisco, which results in a decrease of photosynthetic capacity (Gunderson and Wullschleger, 1993). The average decrease of V_{cmax} among plants in FACE experiments was found to be 13% for all species and 6% for trees (Ainsworth and Long, 2005). Both Wang et al. (1998) and Luo et al. (2001) tested the impact of photosynthetic acclimation and showed a moderate reduction of canopy GPP (5-6%) due to photosynthetic acclimation (10-20%) at the studied experiments.

Following Wang et al. (1998) and Luo et al. (2001), we used MAESPA (Duursma and Medlyn, 2012) to estimate canopy GPP at EucFACE in ambient and elevated C_a treatments. The model has previously been evaluated with leaf- and whole-tree- scale measurements from EucFACE (Yang et al., in review). Here, we first parameterised the model with physiological and structural data measured during the experiment. Then, we

quantified the response of canopy GPP to eC_a and partitioned this response into the direct stimulation of GPP and the indirect effects of photosynthetic acclimation and variation of LAI. The overall goal of this study was to estimate the magnitude of the response of forest canopy GPP to eC_a in order to provide a baseline against which to compare changes in other components of the ecosystem carbon balance.

2. Methods

2.1 Site

The EucFACE experiment (technical details in Gimeno et al., 2015) is located in western Sydney, Australia (33.617S, 150.741E). It consists of six circular plots, each of which has a diameter of 25 m, enclosing 15-25 mature forest trees (referred to as 'rings' hereafter). The rings are divided into two groups: control (with ambient C_a ; 390-400 μmol mol^{-1} during the study period) and experimental (eC_a; +150 μmol mol^{-1}). The tree canopy is dominated by *Eucalyptus tereticornis* Sm. which are ~20 m in height and have a basal area of ~24 m^2 ha^{-1}. The site receives a mean annual precipitation of 800 mm yr^{-1}, a mean annual photosynthetically active radiation (PAR) of 2600 MJ m^{-2} yr^{-1}, and a mean annual temperature of 17 ºC.

2.2 Model

The MAESPA model is a process-based tree-array model (Wang and Jarvis, 1990) that calculates canopy carbon and water exchange (https://bitbucket.org/remkoduursma/maespa/src/Yang_et_al_2019/). At each 30-minute timestep, the model simulates the radiative transfer, photosynthesis, and transpiration of individual trees mechanistically. Soil moisture balance can be calculated dynamically, but here we chose to improve accuracy by using soil moisture as an input to the model (Duursma and Medlyn, 2012).

The model represents the tree canopy as an array of tree crowns. The location and dimensions of each crown are specified based on-site measurements (see 2.3.2 Canopy structure, below). Calculations of carbon and water fluxes are made for each tree crown, which is divided into six layers. Here it was assumed that crowns are represented by an ellipsoidal shape and that leaf area is uniformly distributed across layers within the tree crown. The leaf angles were assumed to follow a spherical distribution to ensure consistency with the method used to estimate leaf area index (LAI) in Duursma et al. (2016). Within each layer, the model evaluates the radiation transfer and leaf gas exchange at 12 grid points such that each crown is represented by a total of 72 grid points. The radiation intercepted at each grid point is calculated for direct and diffuse components by considering shading from the upper crown and surrounding trees and solar angle (zenith and azimuth), and light source (diffuse or direct). Penetration by direct radiation to each grid point is used to estimate the sunlit and shaded leaf area at each grid point. The radiation intercepted by the fraction of sunlit and shade foliage is then used to calculate the leaf gas exchange.

The gas exchange sub-model combines the leaf photosynthesis model of Farquhar et al. (1980) with the stomatal optimisation model, following Medlyn et al. (2011). Stomatal conductance is modelled as:

$$g_s = 1.6 \cdot \left(1 + \frac{g_1}{\sqrt{D}}\right) \cdot \frac{A_{net}}{C_a} \quad (1)$$

where g_s is the stomatal conductance to water vapour (mol m^{-2} s^{-1}); g_1 is a parameter that represents the g_s sensitivity to photosynthesis (kPa$^{0.5}$; see definition in Medlyn et al., (2011)); A_{net} is the net CO_2 assimilation rate

(μmol m^{-2} s^{-1}); C_a is the atmospheric CO_2 concentration (μmol mol^{-1}) and D is the vapour pressure deficit (kPa). The factor 1.6 converts the conductance of CO_2 to that of H_2O.

The impact of soil moisture on g_s is represented through an empirical function that links soil water availability to g_1 following (Drake et al., 2017):

$$g_1 = g_{1.max} \left(\frac{\theta - \theta_{min}}{\theta_{max} - \theta_{min}}\right)^q \quad (2)$$

where the $g_{1.max}$ is the maximum g_1 value; θ is volumetric soil water content (%); θ_{max} and θ_{min} are the upper and lower limit within which θ has impact on g_1; q describes the non-linearity of the curve. The equations to calculate A_{net} are in Supplementary (Text S1, Eqns. S1 – S6).

Following Yang et al. (2019), MAESPA considers a non-stomatal limitation to biochemical parameters J_{max} and V_{cmax} at high D:

$$V_{max} = V_{max.t}(1 - c_D \cdot D) \quad (3)$$

where $V_{max.t}$ is the J_{max} or V_{cmax} at given leaf temperature (Text S1), and c_D is a fitted parameter (Table 1). This relationship is empirical and fitted to data collected in EucFACE. Incorporating this relationship was shown to improve the predicted photosynthesis by the leaf gas exchange model (Yang et al., 2019).

Combining Eqns. 1- 3 and S1 – S6 yields the g_s and A_{net} of each grid point, which is then multiplied by leaf area at each grid point and summed to give whole-tree photosynthesis. Photosynthesis of individual trees is then summed to give whole-canopy photosynthesis.

2.3 Model Parameterisation

2.3.1 Meteorological forcing

The model is driven by *in situ* PAR, wind speed, air temperature, *D*, and soil moisture measurements from 2013 to 2016 (Figures 1 and 2). Each ring has a set of PAR (LI-190, Li-cor, Lincoln, NE, U.S.), wind speed (Wincap Ultrasonic WMT700 Vaisala, Vantaa, Finland), humidity, and temperature sensors (HUMICAP ® HMP 155 Vaisala, Vantaa, Finland) at the centre of the ring above the canopy at 23.5 m. The PAR, air temperature, and relative humidity were measured every five minutes in each ring and then were gap-filled by linear interpolation and aggregated to 30 minute-mean time slices across all six rings (Figure 1). *D* was calculated from temperature and humidity measurements.

Two levels of C_a were used in the model according to the measured C_a (LI-840, Li-cor, Lincoln, NE, U.S.). The ambient C_a was gap-filled (in total <10 days during four years gaps due to power outage) and aggregated to 30 minute-mean time slices from the five-minute measurements across the three ambient rings (rings 2, 3, and 6). The eC_a was processed in the same way but using data from the experimental rings (rings 1, 4, and 5).

The volumetric soil water content (θ) was used as an estimate of plant water availability and was taken every 20 days using neutron measurements at 25 cm intervals (503DR Hydroprobe, Instroteck, NC, U.S.) and averaged to the top 150 cm (Figure 2). There were two probes in each ring and the average of these probes was used to represent the ring average for each measurement date. θ was updated on the days of measurements and thus not gap-filled.

2.3.2 Canopy structure

Trees in MAESPA were represented by their actual location, height, and crown size to mimic the realistic effects of shading. Tree location, crown height, crown base and stem diameter were measured in January 2013 at the start of the experiment. For each ring, a time-series of LAI was obtained based on measurements of above- and below- canopy PAR (Duursma et al. 2016). This LAI represents plant area index, which includes the woody component as well as leaves and does not account for clumping. In order to retrieve the actual LAI, we assumed a constant branch and stem cover (0.8 m^2 m^{-2}) based on the lowest LAI during November 2013 when the canopy shed almost all leaves. The LAI used in this study was thus the plant area index estimates from Duursma et al. (2016), less 0.8 m^2 m^{-2} (Figure 2a). Since LAI is the only parameter beside soil moisture that differed by ring, canopy structure (i.e., the LAI and its distribution) was the major driver of inter-ring variability.

The total leaf area (m^2) of each ring was calculated as the product of LAI and ground area of each plot (491 m^2). This total leaf area (LA) was then assigned to each tree based on an allometric relationship between the total leaf area (m^2) and diameter at breast height (DBH; cm). The allometric relationship was derived from data in the BAAD database (Falster et al., 2015) for *Eucalyptus* trees grown in natural conditions with DBH <1 m to match the characteristics of EucFACE. In total, this database yielded a total of 66 observations with which to estimate the relationship between LA and DBH:

$$L_{allom} = a \cdot DBH^b \quad (4)$$

where L_{allom} is the theoretical leaf area based on allometric relationship to DBH. The values obtained via fitting for a and b were 492.6 and 1.8 respectively, with a root mean square error of 14.4 (m^2) and correlation coefficient of 0.83.. Eqn. 4 was used to assign the total LA of each ring to each tree in the following steps: (i) the L_{allom} for each tree was calculated based on DBH; (ii) the L_{allom} was summed to obtain a total LA for each ring; and (iii) the fractional contribution of each tree to the ring total LA was calculated. The total LA based on LAI was then assigned to each tree based on this fraction.

The crown radius was calculated with a linear function with DBH based on measurements made in August 2016. The data consisted of DBH and crown radius (one on North-South axis and one on East-west axis) of four trees in each ring. The crown radius measurements were averaged by tree and used to fit a linear model with DBH. The estimated slope and intercept of the relationship are 0.095 (m cm^{-1}) and 0.765 (m), respectively.

MAESPA also considered the shading from surrounding trees outside the rings. However, no measurements of locations or diameters were available for the trees surrounding the rings. Therefore, a total of 80 surrounding trees were arbitrarily assumed to form two uniform and circular layers around each ring. They were assigned the mean height, mean crown radius, and mean leaf area estimated from all trees in EucFACE. Except for shading, the surrounding trees have no impact on the trees within the rings. Ring 1 is shown in Figure S1 as an example of the representation of canopy structure in MAESPA.

2.3.3 Physiology

The physiological parameters were estimated from field gas exchange measurements as described below. The data were collected with portable photosynthesis systems (Li-6400, Li-Cor, Inc., USA). The only parameter

found to differ between ambient and elevated C_a rings was $V_{cmax.25}$ (V_{cmax} at 25 ºC; Ellsworth et al., 2017.). Hence, all other parameters (e.g., the temperature responses of photosynthesis and respiration) were estimated by combining all data across CO_2 treatments. Fitted parameter values are given in Table 1.

A set of temperature-controlled photosynthesis-CO_2 response (A-C_i) curves was measured at different leaf temperatures (20-40 ºC) under saturating light in February 2016. The dataset was used to quantify the temperature dependences of J_{max} and V_{cmax} by fitting a peaked Arrhenius function (Eqn. S5) to the measurements. We assumed that these temperature response functions applied throughout the period of the study.

Light- and temperature-controlled A-C_i curves were also measured in the morning for ten field campaigns during 2013 to 2016. All A-C_i curves were started at the growth C_a of 395 μmol mol^{-1} or 545 μmol mol^{-1} (depending on eC_a treatment) with a saturating light of 1800 μmol m^{-2} s^{-1} and a flow rate of 500 μmol s^{-1} with temperature controlled to a constant based on the seasonal temperature. These data were used to estimate J_{max} and V_{cmax} at 25 ºC using the *fitaci* function in the *plantecophys* R package (Duursma, 2015), using the measured temperature responses of J_{max} and V_{cmax} described in the previous paragraph to correct to 25 ºC.

Repeated gas exchange measurements were made on the same leaves in the morning and afternoon under prevailing field conditions and saturating light (photon flux density = 1800 μmol m^{-2} s^{-1}) on four occasions in 2013 ("diurnal"; Gimeno et al., 2015). To expand the diurnal dataset, we obtained the points from A-C_i curves at field C_a and combined the two data sets. These data were used to estimate the g_1 parameter in the stomatal conductance model (Eqn. 1) using the *fitBB* function in the *plantecophys* R package (Duursma, 2015). One g_1 value was fitted to the data from each treatment and date. The g_1 values were then regressed against θ measured in each treatment group to estimate the impact of soil moisture availability on leaf gas exchange, following Eqn. 2. The g_1 values were related to the nearest measurements of θ (within two weeks). There has been no rainfall between g_1 and θ measurement dates. Eqn. 2 was fitted to this data set using the non-linear least squares method (Figure 3).

The dark respiration rate of foliage, R_{dark}, was measured at least three hours after sunset at a range of leaf temperatures (14-60 °C) in February 2016 also with LiCor 6400. The temperature dependence of R_{dark} was fitted using non-linear least squared method to all of the measured data using Eqn. S6. Light responses of photosynthesis were measured on two trees from each ring in October 2014 (Crous et al., unpublished). This data set was used to constrain the light response parameters (α_J and θ_J) in Eqn. S4. Details of fitting the light response curves are provided in supplementary (Text S1).

2.4 Model simulations and analysis

MAESPA was used to simulate radiation interception and gas exchange of all six rings between 1 January 2013 and 31 December 2016 on a half-hourly basis. The model simulated half-hourly gross primary production (GPP) of each tree, which was then summed for all trees in each ring to get the total annual GPP for each ring and year.

Four different sets of simulations were used to estimate carbon uptake under ambient and eC_a and to identify the key limiting factors on canopy GPP response to eC_a. Firstly, we carried out a simulation of leaf scale ("leaf scenario") photosynthesis with measured meteorological data but fixed physiological data (g_1 = 3.3 kPa$^{0.5}$, $V_{cmax.25}$ = 91 μmol m^{-2} s^{-1}, and $J_{max.25}$ = 159 μmol m^{-2} s^{-1}). This simulation aimed to quantify the CO_2 response of

Rubisco-limited and RuBP-limited photosynthesis at the leaf scale. This calculation was made using the *photosyn* function in *plantecophys* R package (Duursma, 2015). This function implements the leaf gas exchange routine used in MAESPA.

Secondly, MAESPA was run for all six rings with ambient C_a and with $V_{cmax.25}$ from ambient measurements ("ambient scenario"). The results of this simulation were used to calculate the GPP of each ring under ambient conditions. The ambient GPP values were also used to evaluate the inherent variability among the rings.

Thirdly, all six rings were simulated with eC_a and $V_{cmax.25}$ based on measurements from ambient rings ("elevated scenario"). The results of this simulation were compared to those from the ambient scenario to illustrate the instantaneous response of canopy GPP to eC_a in each ring and year. This simulation also quantifies the variation of the GPP response to eC_a across rings and years.

Lastly, we simulated the response of the three rings exposed to eC_a (rings 1, 4, and 5) using the $V_{cmax.25}$ and eC_a measured from these elevated rings ("field scenario"). Results from the field scenario were used for two analyses: (i) to compare GPP from the field scenario to that of the three rings from the elevated scenario (i.e., eC_a and ambient $V_{cmax.25}$), which allows us to quantify the impact of photosynthetic acclimation (i.e., due to a reduction in V_{cmax}); (ii) to calculate the difference in GPP between the three ambient rings in ambient scenario and elevated rings in the field scenario to estimate the response of GPP to eC_a in the field.

Table 1. Summary table of parameter definitions, units, and sources used in this study.

Parameters	Definitions	Units	Values	Eqn.
α_J	Quantum yield of electron transport rate	μmol electron μmol^{-1} photon	0.30	S7
a	Fitted slope of LA and DBH	m^2 m^{-1}	492.6	4
a_{abs}	Absorptance of PAR	fraction	0.825	S4
b	Fitted index of LA and DBH	-	1.8	4
c_D	Slope of V_{cmax} to D	kPa^{-1}	0.14	3
ΔS	Entropy factor	J mol^{-1} K^{-1}	639.60 (V_{cmax}); 638.06 (J_{max})	S5
E_a	Activation energy	J mol^{-1}	66386 (V_{cmax}); 32292 (J_{max})	S5
$g_{1.max}$	Maximum g_1 value	kPa$^{0.5}$	5.0	2
H_d	Deactivation energy	J mol^{-1}	200000	S5
θ_J	Convexity of electron transport rate to Q_{APAR}	-	0.48	S8
θ_{max}	Upper limit of soil water content above which g_1 is maximum	-	0.240	2
θ_{min}	Lower limit of soil water content below which g_1 is zero	-	0.106	2
$J_{max.25}$	Value of J_{max} at 25ºC	μmol electron m^{-2} s^{-1}	159	3
k_T	Sensitivity of R_{dark} to temperature	ºC^{-1}	0.078	S6
q	The non-linearity of the g_1 dependence of θ	-	0.425	2
$R_{day.25}$	Light respiration rate	μmol C m^{-2} s^{-1}	0.9	S6
$R_{dark.25}$	Dark respiration rate	μmol C m^{-2} s^{-1}	1.3	S6
R_{gas}	Gas constant	J mol^{-1} K^{-1}	8.314	S5
$V_{cmax.25}$	Value of V_{cmax} at 25ºC	μmol C m^{-2} s^{-1}	91 (ambient); 83 (elevated)	3

3. Results

Figure 4 summarises the results from measurements and the different simulations conducted in this study. It demonstrates that the impact of eC_a diminishes as calculations are scaled from the instantaneous leaf-level response (A_{inst}) to the long-term canopy response (GPP_{field}) and the various feedback effects are accounted for. Each row of Figure 4 is explained in detail in the following paragraphs.

3.1 Instantaneous C_a response of photosynthesis at leaf and canopy scale

The mean instantaneous C_a response of leaf-level photosynthesis (A_{inst}) was +33% (Figure 4a). This response ratio was calculated from ~600 light- and temperature-controlled A-C_i curves measured in the ambient rings. From the curves, we extracted the photosynthesis at 400 and 550 C_a (μmol mol $^{-1}$) and calculated the instantaneous C_a effect as their ratio. This approach allows an estimation of the direct CO_2 response independent of the impact of photosynthetic acclimation.

By contrast, the modelled direct GPP response to eC_a was considerably less, just +11%, as shown in Figure 4d ("GPP_{inst}"). This canopy response rate was calculated by comparing the modelled GPP of all six rings under ambient and elevated C_a ("ambient" vs. "elevated" scenario). As a result, this direct canopy GPP response also excludes the impact of photosynthetic acclimation.

Our results show that the major reason for the difference between the direct leaf and canopy photosynthesis responses to eC_a is the relative contributions from Rubisco- and RuBP-regeneration-limited photosynthesis (cf. Figure 4 b and c). Figure 5 shows that the response of photosynthesis to eC_a is considerably higher when Rubisco activity limits photosynthesis (A_c) than when RuBP-regeneration limits photosynthesis (A_J). When averaged over the range of leaf temperatures experienced during the four years of experiment, the A_c response to eC_a on average (+26%; Figure 4b) is larger than that of A_J (+10%; Figure 4c). Leaf gas exchange measurements were taken in saturating light (1800 μmol m^{-2} s^{-1}) and thus, are mostly Rubisco limited. The observed response rate of A_{inst} is thus close to that of A_c.

At the canopy scale, a large fraction of the modelled canopy photosynthesis is limited by RuBP-regeneration. In Figure 6, we show the distribution of A_c and A_J during the four years of simulation as calculated by MAESPA. On average, 70% of the canopy photosynthesis is limited by RuBP-regeneration under ambient conditions ("ambient scenario"). The high fraction of A_J is partly a consequence of the relatively low ratio of $J_{max.25}$ to $V_{cmax.25}$ (J:V ratio) which was estimated to be 1.7 (Table 1). In Figure 7, we estimated the PAR level at which Rubisco activity becomes limiting to leaf photosynthesis. The transition point from Rubisco- to RuBP-regeneration-limited photosynthesis was calculated from the leaf gas exchange sub-model by assuming a constant C_a (390 μmol mol^{-1}), D (1.5 kPa), g_1 (3.3 kPa$^{0.5}$), and $V_{cmax.25}$ (90 μmol m^{-2} s^{-1}) but varying leaf temperature. As shown, under these conditions, when temperature = 25 ºC and J:V ratio = 1.7, Rubisco activity limits photosynthesis only when incident PAR > 1800 μmol m^{-2} s^{-1}. Using a higher J:V ratio such as the commonly-used value of 2 would decrease the saturating PAR value at which photosynthesis becomes Rubisco limited. We ran additional simulations assuming a J:V ratio of 2 and found that, with this ratio, MAESPA estimated 48% of photosynthesis to be RuBP-regeneration limited under ambient conditions and a direct GPP response of 15% (data not shown).

The shape of the light response curve also determines the transition point from RuBP- to Rubisco-limited photosynthesis. We explored this effect by investigating the effect of varying the convexity, θ_J, which is assumed to be the same as the convexity of overall photosynthesis. At EucFACE, we estimated this parameter as 0.48 from light-response curves of photosynthesis collected on site, indicating a shallow curvature and a high light saturation point, in contrast to the more commonly assumed 0.85, representing a steeper curvature and a lower light saturation point. Using a value of 0.85 for θ_J resulted in a much lower PAR required for photosynthesis to became Rubisco limited (dashed curves in Figure 7). With a θ_J of 0.85 and a J:V ratio of 1.7, MAESPA estimated 40% of photosynthesis to be RuBP-regeneration limited under ambient conditions and a direct GPP response of 16% (data not shown). With a θ_J of 0.85 and a J:V ratio of 2, MAESPA estimated just 34% of photosynthesis to be RuBP-regeneration limited under ambient conditions and a direct GPP response of 18% (Figure S2). The simulated CO_2 response of canopy carbon uptake thus depends heavily on the parameterisation of light response and J:V ratio.

3.2 Acclimation of photosynthesis

The above calculations are made considering only the instantaneous response of photosynthesis to eC_a. However, photosynthetic acclimation was observed at leaf scale (Ellsworth et al., in prep), and will also reduce the response of GPP to eC_a at the canopy scale. At the leaf-level, photosynthesis measured in the elevated rings after five years of treatment (A_{long}) was 19% higher than that measured in ambient rings (Figure 4e; Ellsworth et al. 2017). A_{long} thus accounts for the photosynthetic acclimation in the elevated rings after four years of exposure to eC_a. A_{long} is considerably smaller than A_{inst} (19% vs. 33%; Figure 4 a and e), indicating a large effect of photosynthetic acclimation on the eC_a response of light-saturated photosynthesis.

Accounting for the impact of photosynthetic acclimation in MAESPA, by using the V_{cmax} from elevated rings ("field" vs. "ambient" scenarios) reduced the response of GPP to C_a from 11% to 10% (GPP_{long}; Figure 4f). As such, the photosynthetic acclimation had a relatively modest impact on the modelled annual GPP in the model. The small impact of photosynthetic acclimation on canopy photosynthesis relative to the effect on leaf photosynthesis can be explained by the fact that the leaf photosynthesis data are measured under saturating light and thus are typically Rubisco-limited, so a reduction in V_{cmax} had a large effect. In contrast, at the canopy scale, much of the photosynthesis was limited by RuBP-regeneration and was largely unaffected by a reduction in V_{cmax}.

3.3 Influence of LAI

The realised GPP response to eC_a also depends on the canopy structure, specifically the LAI. In this experiment, there was no significant change in LAI with eC_a (-4% ± 5%; Figure 4g; see also Duursma et al. 2016). The effect of eC_a on LAI was calculated as the average effect between elevated and ambient annual mean LAI. However, there was inherent variability in LAI across the rings (Figure 2a), which does not fundamentally change the effect of eC_a but requires a detailed analysis of the potential effects of natural variability on the response to eC_a.

The small pre-treatment difference in LAI across rings gives rise to a range of estimates for the GPP response to eC_a in the field (6% ±8%; Figure 4h). This result is explored further in Figure 8, which combines the results from "ambient", "elevated", and "field" scenarios. The average GPP across all six rings under ambient C_a was 1574 g C m^{-2} yr^{-1} over the four-year simulation ("ambient scenario"; Figure 8). However, there was significant variability in ambient GPP across rings, related in part to the inherent variability in LAI across rings. We characterised the pre-existing differences in LAI by the initial LAI (LAI_i), measured on 26 October 2012. These initial values are low, because they are measured immediately before the seasonal leaf flush, but characterise the difference in LAI across rings over the full experimental period. Rings 1 and 4 (both experimental rings) have the lowest LAI_i (<0.3 m^2 m^{-2}) and thus the lowest average GPP under ambient conditions (1206 g C m^{-2} yr^{-1}). Ring 5 (the other experimental ring) has the second highest LAI_i (~0.4 m^2 m^{-2}) and also the highest GPP under ambient conditions (2359 g C m^{-2} yr^{-1}). The variability among rings in ambient GPP (SD = 15%) is thus larger than the modelled direct effect of C_a on GPP, which is similar in all rings (+11%).

Owing to the variability among rings represented by LAI_i, the estimated mean GPP response to eC_a across the experimental rings has a sizeable confidence interval (±8%, Figure 4h). The actual eC_a response was estimated as an average effect between the ambient and elevated GPP values considering the impacts of photosynthetic acclimation and inter-ring variability. The average GPP of experimental rings under field conditions (eC_a) was estimated to be 1698 g C m^{-2} yr^{-1} while the average GPP of control rings under field conditions (ambient C_a) was 1599 g C m^{-2} yr^{-1}, an increase of 6% as shown in the Figure 4h. The variation of annual average GPP of the control and experimental groups (blue and red squares in Figure 8) are thus represented by the CI in Figure 4h.

4. Discussion

We have showed how a large response of leaf-level photosynthesis to eC_a diminishes when integrated to the canopy-scale, according to the synthesis of four years of leaf measurements at EucFACE with the stand-scale model, MAESPA. We estimated that the canopy GPP of a mature *Eucalyptus* woodland under ambient C_a conditions varied from 1084–2129 g C m^{-2} yr^{-1} by ring and year with a mean of 1574 g C m^{-2} yr^{-1}. The model, constrained by site measurements, predicted that once scaled to the canopy, the response of GPP to eC_a only increased by 6% (95% CI of ±8%) compared to the 19% (95% CI of ±5%) observed in leaf-scale measurements. We were able to quantify the response of GPP to eC_a and attribute the reduction in the response to various factors including: (i) Rubisco versus RuBP-regeneration limitations to photosynthesis; (ii) photosynthetic acclimation; (iii) inter-ring variability in LAI. Together these findings provide valuable insights into the relative importance of each factor and help close a key knowledge gap in our understanding of how mature forests respond to eC_a.

4.1 Performance of MAESPA under ambient conditions

The ambient GPP of EucFACE estimated by MAESPA was comparable to that measured with eddy covariance in similar evergreen Eucalypt forests in Southeast Australia. In a nearby eddy covariance site (<1 km), , Renchon et al. (2018) estimated the ecosystem GPP from eddy convariance to be 1561 g C m^{-2} yr^{-1} during 2013 to 2016 which is within the range estimated for the ambient rings in this study, though this latter site and the EucFACE are not the same in terms of canopy structure and LAI. Furthermore, our version of MAESPA was

evaluated against leaf photosynthesis and whole-tree sap flow measurements in EucFACE (R^2 of 0.77 and 0.8, respectively; Yang et al., 2019). These comparisons indicate MAESPA is a useful tool to explore the canopy carbon uptake and the predicted GPP could provide a baseline to future studies.

4.2 RuBP-regeneration limited photosynthesis

Our results show that the canopy GPP at EucFACE was predominantly limited by RuBP regeneration. The reason for the frequent RuBP-regeneration limitation is that the measured J:V ratio was relatively small in EucFACE (1.7), and stomata tend to close at midday when light levels are higher and Rubisco-limitation is expected (Gimeno et al., 2015). A lower J:V ratio increases the PAR threshold required for the photosynthesis model to switch between the RuBP-regeneration limitation and the Rubisco limitation (from <1000 to <1800 μmol m^{-2} s^{-1}; Figure 7). Previous studies have highlighted the need to consider J:V ratio for a correct prediction of CO_2 response (Long et al, 2004; Zaehle et al., 2014; Rogers et al., 2017). However, as shown by Zaehle et al. (2014), Medlyn et al. (2015), and Rogers et al. (2017), current models differ in their predictions of the transition from RuBP-regeneration- to Rubisco-limited photosynthesis, suggesting the uncertainty of predicted CO_2 response of GPP could be reduced by using a realistic J:V ratio.

Previous modelling studies applying MAESPA to eC_a experiments both assumed higher J:V ratio (2) and estimated higher GPP response to eC_a presumably due to less frequent RuBP-regeneration limitation (Wang et al., 1998; Luo et al., 2001). A J:V ratio of 2 was suggested by Wullschleger (1993) and has been used in many modelling studies (e.g., the seven terrestrial biosphere models assessed by Rogers et al. (2017) all assumed a J:V ratio of 1.9-2). Global terrestrial biosphere models such as JULES and others frequently estimate J_{max} on the basis of this ratio (e.g., Clark et al. 2011). However, the relatively low J:V ratio observed at EucFACE is not unique. At the Duke Forest FACE site in the US, Ellsworth et al. (2012) reported a J:V ratio of ~1.7 which is the same as that estimated for EucFACE. Kattge and Knorr (2007) analysed V_{cmax} and J_{max} values from 36 species across the world and found a low J:V ratio (<1.8) in herbaceous, coniferous, and broadleaved species. Most recently, Kumarathunge et al. (2018) studied the variation in J:V ratio in datasets obtained from around the globe and found that it declined with increasing growing season temperature. The ratio varied from 2.5 in tundra environments to < 1.5 in tropical environments. The value of 1.7 observed at EucFACE falls within this prediction for the prevailing growth temperature at this site. The inclusion of this relationship between J:V ratio and temperature will thus be important for capturing the GPP response to eC_a globally.

We also found that the convexity of the light response of photosynthesis affected the predicted GPP response to eC_a (Figure 7). The parameter value we fitted to data measured *in situ* (θ_J = 0.48) is lower than the value commonly assumed in the models (e.g., 0.7 in Bonan et al., 2011). Note that some model studies assume that θ_J to be lower than the convexity of overall photosynthesis (typically over 0.8; e.g., 0.9 in Medlyn et al., 2002; 0.85 in Haverd et al., 2018). Here we assumed that the convexity of electron transport rate and overall photosynthesis are the same (see Supplementary Text S1 for details). Nonetheless, our relatively low θ_J value (<0.7) is not unique, as it is also supported by a number of studies on different species around the world (Ögren, 1993; Valladares et al., 1997; Lewis et al., 2000; Hjelm and Ögren, 2004). The inclusion of higher θ_J value would predict a much higher direct GPP response to eC_a (e.g., 16% versus 11% in this study), because higher θ_J results in a large proportion of GPP being Rubisco-limited. This finding calls for careful examination of the light-response of photosynthesis, which has a large effect on the predicted eC_a response

4.2 Photosynthetic acclimation

Some degree of photosynthetic acclimation (i.e., a long-term reduction of V_{cmax} under eC_a) has been widely reported in FACE studies and has been attributed to a reduction of leaf nitrogen concentration (Saxe et al., 1998; Ainsworth and Long, 2005). The response of GPP to eC_a would be linearly related to V_{cmax} if photosynthesis were mostly limited by Rubisco activity. Photosynthetic acclimation was responsible for the reduced response of leaf-scale light-saturated photosynthesis from 33% (A_{inst}) to 19% (A_{long}). However, this reduction in V_{cmax} translated into only a ~2% reduction in GPP modelled by MAESPA. Wang et al. (1998) also showed that photosynthetic acclimation (-21% in V_{cmax}) reduced modelled canopy GPP by only 6% due to RuBP-regeneration being the primary limitation of canopy photosynthesis. These findings thus suggest that photosynthetic acclimation may only have a small effect in the GPP response to eC_a when canopy photosynthesis is mostly RuBP-regeneration limited. This response is thus consistent with the hypothesis that the reduction in V_{cmax} represents a re-allocation of nitrogen to optimise nitrogen use efficiency under eC_a (Chen et al., 1993; Medlyn et al., 1996).

4.3 Constraining the carbon balance response to eC_a

At EucFACE, after four years of eC_a treatment, there was no evidence of increased above-ground tree growth (Ellsworth et al., 2017). Nor have the trees at EucFACE shown any significant change in LAI (Duursma et al., 2016). The relatively small response of GPP and the effect of ring-to-ring variation provides important context for these statistically non-significant responses of tree growth at the stand scale at EucFACE. Firstly, the effect size calculated for GPP of +11% (+ 169 g C m^{-2} yr^{-1}) constrains the likely effect size for plant growth and other components of the ecosystem carbon balance and is a more useful baseline for comparison than the response of light-saturated leaf photosynthesis (+19% = 299 g C).

Secondly, the inherent ring-to-ring variation in this natural forest stand is larger than the GPP response, which highlights the importance of considering both the effect size and variability in the observations than to focus on statistical significance. It is important to note that the EucFACE site could be considered relatively homogeneous for a mature woodland. The site is flat, trees appear similar-aged, and almost all the overstory belongs to a single species. In addition, plots were carefully sited to minimise variation in basal area. However, there are small-scale variations in soil type, depth, and nutrient availability that cause variation in LAI. This scale of variation is likely to present in other natural forests, and indeed, other studies on mature trees also note that background variability can contribute to the lack of statistically significant findings (Fatichi and Leuzinger, 2013; Sigurdsson et al. 2013). We highlight the need to focus on effect size and its uncertainty, rather than the dichotomous significant/non-significant approach when evaluating experimental results from native forests.

4.4 Implications for terrestrial biosphere models

Seven Terrestrial Biosphere Models (TBMs) were used to predict GPP and LAI responses to eC_a in advance of the EucFACE experiment (Medlyn et al. 2016). The predicted eC_a responses of GPP ranged from +2 to +24% across the seven models, while the predicted responses of LAI ranged from +1 to +20%. With our results, it is possible to falsify some of the assumptions made in these model simulations and identify directions for model improvement. The model with the lowest GPP response (CLM4-P) assumed very strong down-regulation of photosynthesis owing to phosphorus limitation. However, this down-regulation was not observed here. The

models with the highest GPP responses (GDAY, O-CN, SDGVM) had a J:V ratio of 2 which is higher than that observed at EucFACE, and also had a positive feedback to GPP via increased LAI (+5-15%), which did not occur (Duursma et al., 2016). The model rendering most similar prediction for the GPP response to eC_a to the output of MAESPA incorporating empirical observations was the CABLE model. This latter model predicted an eC_a response of GPP of ~12% with a large proportion of RuBP-regeneration limited photosynthesis, both of which are similar to the findings in this study. Future TBMs may benefit from incorporating a more realistic representation of the relative contribution of RuBP-regeneration- to Rubisco- limited photosynthesis to GPP. For instance, adding the temperature dependency of J:V ratio could help capture the variation of J:V ratio globally (e.g., Kumarathunge et al., 2018).

Our study provides a number of process-based insights that can be used to improve model performance both qualitatively and quantitatively. Our modelling exercise is also a major contribution to the understanding of the EucFACE experiment by quantifying the amount of extra carbon input into the system by canopy-level photosynthesis and thus providing a reference for assessing the impacts of eC_a on growth and soil respiration. Finally, our study highlights that the eC_a effect on canopy-scale GPP may be considerably lower than the effect on photosynthesis of the light-saturated leaves, due to contrasting relative limitations to photosynthesis operating and different scales. In future work, our GPP estimates will be used as an input to calculate the overall effect of eC_a on the carbon balance at the whole EucFACE site.

Acknowledgements

JY was supported by a PhD scholarship from Hawkesbury Institute for the Environment, Western Sydney University. MGDK was supported by NSW Research Attraction and Acceleration Program (RAAP).

EucFACE was built as an initiative of the Australian Government as part of the Nation-building Economic Stimulus Package and is supported by the Australian Commonwealth in collaboration with Western Sydney University. It is also part of a TERN Super-site facility.

We thank Vinod Kumar, Craig McNamara and Craig Barton, for their excellent technical support. We also thank Elise Dando for help in measuring crown radius, Steven Wohl for crane driving, Julia Cooke and Burhan Amiji for installing the neutron probe access tubes.

Author contribution statement

JY, BM, MDK, and RD conceived and designed the analysis. KC, DE, and TG designed sampling of leaf physiological data, while DE and RD designed sampling of canopy structure data. KC, DE, TG, AWK, RD and JY collected data. RD and DK provided analysis tools. JY and BM performed the analysis. JY, BM, MDK, and MJ wrote the paper. All authors edited and approved the manuscript.

References

Ainsworth, E. A. and Long, S. P.: What have we learned from 15 years of free-air CO_2 enrichment (FACE)? A meta-analytic review of the responses of photosynthesis, canopy properties and plant production to rising CO_2, *New Phytol.*, 165(2), 351–372, doi:10.1111/j.1469-8137.2004.01224.x, 2005.

Bernacchi, C. J., Singsaas, E. L., Pimentel, C., Portis Jr, A. R. and Long, S. P.: Improved temperature response functions for models of Rubisco-limited photosynthesis, *Plant, Cell Environ.*, 24(2), 253–259, doi:10.1046/j.1365-3040.2001.00668.x, 2001.

Bonan, G. B. and Doney, S. C.: Climate, ecosystems, and planetary futures: The challenge to predict life in Earth system models, *Science* (80-)., 359(6375), doi:10.1126/science.aam8328, 2018.

Bonan, G. B., Lawrence, P. J., Oleson, K. W., Levis, S., Jung, M., Reichstein, M., Lawrence, D. M. and Swenson, S. C.: Improving canopy processes in the Community Land Model version 4 (CLM4) using global flux fields empirically inferred from FLUXNET data, *J. Geophys. Res.*, 116(G2), 1–22, doi:10.1029/2010jg001593, 2011.

Chen, J. L., Reynolds, J. F., Harley, P. C. and Tenhunen, J. D.: Coordination theory of leaf nitrogen distribution in a canopy, *Oecologia*, 93(1), 63–69, doi:10.1007/BF00321192, 1993.

Clark, D. B., Mercado, L. M., Sitch, S., Jones, C. D., Gedney, N., Best, M. J., Pryor, M., Rooney, G. G., Essery, R. L. H., Blyth, E., Boucher, O., Harding, R. J., Huntingford, C. and Cox, P. M.: The Joint UK Land Environment Simulator (JULES), model description – Part 2: Carbon fluxes and vegetation dynamics, *Geosci. Model Dev.*, 4(3), 701–722, doi:10.5194/gmd-4-701-2011, 2011.

Curtis, P. S., and X. Wang (1998), A meta-analysis of elevated CO_2 effects on woody plant mass, form, and physiology, Oecologia, 113(3), 299–313, doi:10.1007/s004420050381.

Dawes, M. A., Hättenschwiler, S., Bebi, P., Hagedorn, F., Handa, I. T., Körner, C. and Rixen, C.: Species-specific tree growth responses to 9 years of CO_2 enrichment at the alpine treeline, *J. Ecol.*, 99(2), 383–394, doi:10.1111/j.1365-2745.2010.01764.x, 2011.

De Kauwe, M. G., Medlyn, B. E., Zaehle, S., Walker, A. P., Dietze, M. C., Wang, Y. P., Luo, Y., Jain, A. K., El-Masri, B., Hickler, T., Wårlind, D., Weng, E., Parton, W. J., Thornton, P. E., Wang, S., Prentice, I. C., Asao, S., Smith, B., Mccarthy, H. R., Iversen, C. M., Hanson, P. J., Warren, J. M., Oren, R. and Norby, R. J.: Where does the carbon go? A model-data intercomparison of vegetation carbon allocation and turnover processes at two temperate forest free-air CO_2 enrichment sites, *New Phytol.*, 203(3), 883–899, doi:10.1111/nph.12847, 2014.

Donohue, R. J., Mcvicar, T. R. and Roderick, M. L.: Climate-related trends in Australian vegetation cover as inferred from satellite observations, 1981-2006, *Glob. Chang. Biol.*, 15(4), 1025–1039, doi:10.1111/j.1365-2486.2008.01746.x, 2009.

Donohue, R. J., Roderick, M. L., McVicar, T. R. and Farquhar, G. D.: Impact of CO_2 fertilization on maximum foliage cover across the globe's warm, arid environments, *Geophys. Res. Lett.*, 40(12), 3031–3035, doi:10.1002/grl.50563, 2013.

Drake, J. E., Power, S. A., Duursma, R. A., Medlyn, B. E., Aspinwall, M. J., Choat, B., Creek, D., Eamus, D., Maier, C., Pfautsch, S., Smith, R. A., Tjoelker, M. G. and Tissue, D. T.: Stomatal and non-stomatal limitations of photosynthesis for four tree species under drought: A comparison of model formulations, *Agric. For. Meteorol.*, 247, 454–466, doi:10.1016/j.agrformet.2017.08.026, 2017.

Duursma, R. A. and Medlyn, B. E.: MAESPA: a model to study interactions between water limitation, environmental drivers and vegetation function at tree and stand levels, with an example application to $[CO_2] \times$ drought interactions, *Geosci. Model Dev.*, 5(4), 919–940, doi:10.5194/gmd-5-919-2012, 2012.

Duursma, R. A.: Plantecophys - An R package for analysing and modelling leaf gas exchange data, *PLoS One*, 10(11), 1–13, doi:10.1371/journal.pone.0143346, 2015.

549 Duursma, R. A., Gimeno, T. E., Boer, M. M., Crous, K. Y., Tjoelker, M. G. and Ellsworth, D. S.: Canopy leaf
550 area of a mature evergreen *Eucalyptus* woodland does not respond to elevated atmospheric [CO_2] but tracks
551 water availability, *Glob. Chang. Biol*., 22(4), 1666–1676, doi:10.1111/gcb.13151, 2016.

552 Eamus, D. and Jarvis, P. G.: The direct effects of increase in the global atmospheric co_2 concentration on natural
553 and commercial temperate trees and forests, *Advances in Ecological Research*, vol. 19, pp. 1–55., 1989.

554 Ellsworth, D. S., Thomas, R., Crous, K. Y., Palmroth, S., Ward, E., Maier, C., Delucia, E. and Oren, R.:
555 Elevated CO_2 affects photosynthetic responses in canopy pine and subcanopy deciduous trees over 10 years: A
556 synthesis from Duke FACE, *Glob. Chang. Biol*., 18(1), 223–242, doi:10.1111/j.1365-2486.2011.02505.x, 2012.

557 Ellsworth, D. S., Anderson, I. C., Crous, K. Y., Cooke, J., Drake, J. E., Gherlenda, A. N., Gimeno, T. E.,
558 Macdonald, C. A., Medlyn, B. E., Powell, J. R., Tjoelker, M. G. and Reich, P. B.: Elevated CO_2 does not
559 increase eucalypt forest productivity on a low-phosphorus soil, *Nat. Clim. Chang*., 7(4), 279–282,
560 doi:10.1038/nclimate3235, 2017.

561 Farquhar, G. D., Caemmerer, S. and Berry, J. A.: A biochemical model of photosynthetic CO_2 assimilation in
562 leaves of C3 species, *Planta*, 149(1), 78–90, doi:10.1007/BF00386231, 1980.

563 Fatichi, S. and Leuzinger, S.: Reconciling observations with modeling: The fate of water and carbon allocation
564 in a mature deciduous forest exposed to elevated CO_2, *Agric. For. Meteorol.*, 174–175, 144–157,
565 doi:10.1016/j.agrformet.2013.02.005, 2013.

566 Fatichi, S., Pappas, C., Zscheischler, J. and Leuzinger, S.: Modelling carbon sources and sinks in terrestrial
567 vegetation, *New Phytol*., 221(2), 652–668, doi:10.1111/nph.15451, 2019.

568 Friend, A.: Modelling canopy CO_2 fluxes: are 'big-leaf' simplifications justified?, Glob. Ecol. Biogeogr., 10(6),
569 603–619, 2001.

570 Gimeno, T. E., Crous, K. Y., Cooke, J., O'Grady, A. P., Ósvaldsson, A., Medlyn, B. E. and Ellsworth, D. S.:
571 Conserved stomatal behaviour under elevated CO_2 and varying water availability in a mature woodland, *Funct.*
572 *Ecol*., 30(5), 700–709, doi:10.1111/1365-2435.12532, 2016.

573 Gimeno, T. E., McVicar, T. R., O'Grady, A. P., Tissue, D. T. and Ellsworth, D. S.: Elevated CO_2 did not affect
574 the hydrological balance of a mature native *Eucalyptus* woodland, *Glob. Chang. Biol.*, 33(0), 0–2,
575 doi:10.1111/gcb.14139, 2018.

576 Haverd, V., Smith, B., Nieradzik, L., Briggs, P. R., Woodgate, W., Trudinger, C. M., Canadell, J. G. and Cuntz,
577 M.: A new version of the CABLE land surface model (Subversion revision r4601) incorporating land use and
578 land cover change, woody vegetation demography, and a novel optimisation-based approach to plant
579 coordination of photosynthesis, Geosci. Model Dev., 11(7), 2995–3026, doi:10.5194/gmd-11-2995-2018, 2018.

580 Hjelm, U. and Ögren, E.: Photosynthetic responses to short-term and long-term light variation in Pinus
581 sylvestris and Salix dasyclados, Trees, 18(6), 622–629, doi:10.1007/s00468-004-0329-8, 2004.

582 IPCC, 2014: Climate Change 2014: Synthesis Report. Contribution of Working Groups I, II and III to the Fifth
583 Assessment Report of the Intergovernmental Panel on Climate Change [Core Writing Team, R.K. Pachauri and
584 L.A. Meyer (eds.)]. *IPCC*, Geneva, Switzerland, 151 pp.

585 Joos, F. and Spahni, R.: Rates of change in natural and anthropogenic radiative forcing over the past 20,000
586 years, *Proc. Natl. Acad. Sci*., 105(5), 1425–1430, doi:10.1073/pnas.0707386105, 2008.

587 Knauer, J., Zaehle, S., De Kauwe, M. G., Bahar, N. H. A., Evans, J. R., Medlyn, B. E., Reichstein, M. and
588 Werner, C.: Effects of mesophyll conductance on vegetation responses to elevated CO_2 concentrations in a land
589 surface model, *Glob. Chang. Biol*., (September 2018), 1–19, doi:10.1111/gcb.14604, 2019.

590 Keenan, T. F., Hollinger, D. Y., Bohrer, G., Dragoni, D., Munger, J. W., Schmid, H. P. and Richardson, A. D.:
591 Increase in forest water-use efficiency as atmospheric carbon dioxide concentrations rise, *Nature*, 499(7458),
592 324–327, doi:10.1038/nature12291, 2013.

593 Kimball, B. A., Mauney, J. R., Nakayama, F. S. I. and Idso, S. B.: Effects of increasing atmospheric CO_2 on
594 vegetation, *Vegetatio*, 104/105, 65–75 [online] Available from:
595 https://link.springer.com/article/10.1007/BF00048145, 1993.

596 Klein, T., Bader, M. K. F., Leuzinger, S., Mildner, M., Schleppi, P., Siegwolf, R. T. W. and Körner, C.: Growth
597 and carbon relations of mature *Picea abies* trees under 5 years of free-air CO_2 enrichment, edited by E. Lines, *J.*
598 *Ecol.*, 104(6), 1720–1733, doi:10.1111/1365-2745.12621, 2016.

599 Körner, C., Asshoff, R., Bignucolo, O., Hattenschwiler, S., Keel, S. G., Pelaez-Riedl, S., Pepin, S., Siegwolf, R.
600 T. W. and Zotz, G.: Carbon flux and growth in mature deciduous forest trees exposed to elevated CO_2, *Science*
601 (80)., 309(5739), 1360–1362, 2005.

602 Kumarathunge, D. P., Medlyn, B. E., Drake, J. E., Tjoelker, M. G., Aspinwall, M. J., Battaglia, M., Cano, F. J.,
603 Carter, K. R., Cavaleri, M. A., Cernusak, L. A., Chambers, J. Q., Crous, K. Y., De Kauwe, M. G., Dillaway, D.
604 N., Dreyer, E., Ellsworth, D. S., Ghannoum, O., Han, Q., Hikosaka, K., Jensen, A. M., Kelly, J. W. G., Kruger,
605 E. L., Mercado, L. M., Onoda, Y., Reich, P. B., Rogers, A., Slot, M., Smith, N. G., Tarvainen, L., Tissue, D. T.,
606 Togashi, H. F., Tribuzy, E. S., Uddling, J., Vårhammar, A., Wallin, G., Warren, J. M. and Way, D. A.:
607 Acclimation and adaptation components of the temperature dependence of plant photosynthesis at the global
608 scale, *New Phytol.*, 222(2), 768–784, doi:10.1111/nph.15668, 2019.

609 Le Quéré, C., Andrew, R. M., Friedlingstein, P., Sitch, S., Pongratz, J., Manning, A. C., Korsbakken, J. I.,
610 Peters, G. P., Canadell, J. G., Jackson, R. B., Boden, T. A., Tans, P. P., Andrews, O. D., Arora, V. K., Bakker,
611 D. C. E., Barbero, L., Becker, M., Betts, R. A., Bopp, L., Chevallier, F., Chini, L. P., Ciais, P., Cosca, C. E.,
612 Cross, J., Currie, K., Gasser, T., Harris, I., Hauck, J., Haverd, V., Houghton, R. A., Hunt, C. W., Hurtt, G.,
613 Ilyina, T., Jain, A. K., Kato, E., Kautz, M., Keeling, R. F., Klein Goldewijk, K., Körtzinger, A., Landschützer,
614 P., Lefèvre, N., Lenton, A., Lienert, S., Lima, I., Lombardozzi, D., Metzl, N., Millero, F., Monteiro, P. M. S.,
615 Munro, D. R., Nabel, J. E. M. S., Nakaoka, S., Nojiri, Y., Padín, X. A., Peregon, A., Pfeil, B., Pierrot, D.,
616 Poulter, B., Rehder, G., Reimer, J., Rödenbeck, C., Schwinger, J., Séférian, R., Skjelvan, I., Stocker, B. D.,
617 Tian, H., Tilbrook, B., van der Laan-Luijkx, I. T., van der Werf, G. R., van Heuven, S., Viovy, N., Vuichard, N.,
618 Walker, A. P., Watson, A. J., Wiltshire, A. J., Zaehle, S. and Zhu, D.: Global Carbon Budget 2017, *Earth Syst.*
619 *Sci. Data Discuss.*, (November), 1–79, doi:10.5194/essd-2017-123, 2017.

620 Lewis, J. D., McKane, R. B., Tingey, D. T. and Beedlow, P. A.: Vertical gradients in photosynthetic light
621 response within an old-growth Douglas-fir and western hemlock canopy, Tree Physiol., 20(7), 447–456,
622 doi:10.1093/treephys/20.7.447, 2000.

623 Long, S. P., Ainsworth, E. A., Rogers, A. and Ort, D. R.: Rising atmospheric carbon dioxide: Plants FACE the
624 Future, *Annu. Rev. Plant Biol.*, 55(1), 591–628, doi:10.1146/annurev.arplant.55.031903.141610, 2004.

625 Luo, Y., Medlyn, B., Hui, D., Ellsworth, D., Reynolds, J. and Katul, G.: Gross primary productivity in duke
626 forest: Modeling synthesis of CO_2 experiment and eddy-flux data, *Ecol. Appl.*, 11(1), 239–252,
627 doi:10.2307/3061070, 2001.

628 Medlyn, B. E.: Interactive effects of atmospheric carbon dioxide and leaf nitrogen concentration on canopy light
629 use efficiency: A modeling analysis, *Tree Physiol.*, 16(1–2), 201–209, doi:10.1093/treephys/16.1-2.201, 1996.

630 Medlyn, B., Badeck, F.-W., De Pury, D., Barton, C., Broadmeadow, M., Ceulemans, R., De Angelis, P.,
631 Forstreuter, M., Jach, M., Kellomäki, S., Laitat, E., Marek, M., Philippot, S., Rey, A., Strassemeyer, J., Laitinen,
632 K., Liozon, R., Portier, B., Robertntz, P., Wang, K. and Jarvis, P.: Effects of elevated [CO_2] on photosynthesis
633 in European forest species: a meta-analysis of model parameters, *Plant Cell Environ.*, 22, 1475–1495, 1999.

Medlyn, B. E., De Kauwe, M. G., Zaehle, S., Walker, A. P., Duursma, R. A., Luus, K., Mishurov, M., Pak, B., Smith, B., Wang, Y. P., Yang, X., Crous, K. Y., Drake, J. E., Gimeno, T. E., Macdonald, C. A., Norby, R. J., Power, S. A., Tjoelker, M. G. and Ellsworth, D. S.: Using models to guide field experiments: *a priori* predictions for the CO_2 response of a nutrient- and water-limited native *Eucalypt* woodland, *Glob. Chang. Biol*., 22(8), 2834–2851, doi:10.1111/gcb.13268, 2016.

Medlyn, B. E., Dreyer, E., Ellsworth, D., Forstreuter, M., Harley, P. C., Kirschbaum, M. U. F., Le Roux, X., Montpied, P., Strassemeyer, J., Walcroft, a., Wang, K. and Loustau, D.: Temperature response of parameters of a biochemically based model of photosynthesis. II. A review of experimental data, *Plant, Cell Environ*., 25(9), 1167–1179, doi:10.1046/j.1365-3040.2002.00891.x, 2002.

Medlyn, B. E., Duursma, R. A., Eamus, D., Ellsworth, D. S., Prentice, I. C., Barton, C. V. M., Crous, K. Y., De Angelis, P., Freeman, M. and Wingate, L.: Reconciling the optimal and empirical approaches to modelling stomatal conductance, *Glob. Chang. Biol*., 17(6), 2134–2144, doi:10.1111/j.1365-2486.2010.02375.x, 2011.

Medlyn, B. E., Zaehle, S., De Kauwe, M. G., Walker, A. P., Dietze, M. C., Hanson, P. J., Hickler, T., Jain, A. K., Luo, Y., Parton, W., Prentice, I. C., Thornton, P. E., Wang, S., Wang, Y. P., Weng, E., Iversen, C. M., Mccarthy, H. R., Warren, J. M., Oren, R. and Norby, R. J.: Using ecosystem experiments to improve vegetation models, *Nat. Clim. Chang*., 5(6), 528–534, doi:10.1038/nclimate2621, 2015.

Morison, J. I. L.: Sensitivity of stomata and water use efficiency to high CO_2, Plant, Cell Environ., 8, 467–474, 1985.Niinemets, Ü., Keenan, T. F. and Hallik, L.: A worldwide analysis of within-canopy variations in leaf structural, chemical and physiological traits across plant functional types, *New Phytol*., 205(3), 973–993, doi:10.1111/nph.13096, 2015.

Norby, R. J., DeLucia, E. H., Gielen, B., Calfapietra, C., Giardina, C. P., King, J. S., Ledford, J., McCarthy, H. R., Moore, D. J. P., Ceulemans, R., De Angelis, P., Finzi, A. C., Karnosky, D. F., Kubiske, M. E., Lukac, M., Pregitzer, K. S., Scarascia-Mugnozza, G. E., Schlesinger, W. H. and Oren, R.: Forest response to elevated CO_2 is conserved across a broad range of productivity, *Proc. Natl. Acad. Sci*., 102(50), 18052–18056, doi:10.1073/pnas.0509478102, 2005.

Ögren, E.: Convexity of the Photosynthetic Light-Response Curve in Relation to Intensity and Direction of Light during Growth., Plant Physiol., 101(3), 1013–1019 [online] Available from: http://www.ncbi.nlm.nih.gov/pubmed/12231754%0Ahttp://www.pubmedcentral.nih.gov/articlerender.fcgi?artid=PMC158720, 1993.

Pan, Y., Birdsey, R. A., Fang, J., Houghton, R., Kauppi, P. E., Kurz, W. A., Phillips, O. L., Shvidenko, A., Lewis, S. L., Canadell, J. G., Ciais, P., Jackson, R. B., Pacala, S. W., McGuire, A. D., Piao, S., Rautiainen, A., Sitch, S. and Hayes, D.: A large and persistent carbon sink in the world's forests, *Science* (80)., 333(6045), 988–993, doi:10.1126/science.1201609, 2011.

Peñuelas, J., Canadell, J. G. and Ogaya, R.: Increased water-use efficiency during the 20th century did not translate into enhanced tree growth, *Glob. Ecol. Biogeogr*., 20(4), 597–608, doi:10.1111/j.1466-8238.2010.00608.x, 2011.

Renchon, A. A., Griebel, A., Metzen, D., Williams, C. A., Medlyn, B., Duursma, R. A., Barton, C. V. M., Maier, C., Boer, M. M., Isaac, P., Tissue, D., Resco De DIos, V. and Pendall, E.: Upside-down fluxes Down Under: CO2net sink in winter and net source in summer in a temperate evergreen broadleaf forest, *Biogeosciences*, 15(12), 3703–3716, doi:10.5194/bg-15-3703-2018, 2018.

Saxe, H., Ellsworth, D. S. and Heath, J.: Tree and forest functioning in an enriched CO_2 atmosphere, *New Phytol*., 139(3), 395–436, doi:10.1046/j.1469-8137.1998.00221.x, 1998.

Sigurdsson, B. D., Medhurst, J. L., Wallin, G., Eggertsson, O. and Linder, S.: Growth of mature boreal Norway spruce was not affected by elevated [CO_2] and/or air temperature unless nutrient availability was improved, *Tree Physiol.*, 33(11), 1192–1205, doi:10.1093/treephys/tpt043, 2013.

Silva, L. C. R. and Anand, M.: Probing for the influence of atmospheric CO_2 and climate change on forest ecosystems across biomes, *Glob. Ecol. Biogeogr.*, 22(1), 83–92, doi:10.1111/j.1466-8238.2012.00783.x, 2013.

Slevin, D., Tett, S. F. B. and Williams, M.: Multi-site evaluation of the JULES land surface model using global and local data, *Geosci. Model Dev.*, 8(2), 295–316, doi:10.5194/gmd-8-295-2015, 2015.

Valladares, F., Allen, M. T. and Pearcy, R. W.: Photosynthetic responses to dynamic light under field conditions in six tropical rainforest shrubs occurring along a light gradient, Oecologia, 111(4), 505–514, doi:10.1007/s004420050264, 1997.

van der Sleen, P., Groenendijk, P., Vlam, M., Anten, N. P. R., Boom, A., Bongers, F., Pons, T. L., Terburg, G. and Zuidema, P. A.: No growth stimulation of tropical trees by 150 years of CO_2 fertilization but water-use efficiency increased, *Nat. Geosci.*, 8(1), 24–28, doi:10.1038/ngeo2313, 2015.

Walker, A. P., De Kauwe, M. G., Medlyn, B. E., Zaehle, S., Iversen, C. M., Asao, S., Guenet, B., Harper, A., Hickler, T., Hungate, B. A., Jain, A. K., Luo, Y., Lu, X., Lu, M., Luus, K., Megonigal, J. P., Oren, R., Ryan, E., Shu, S., Talhelm, A., Wang, Y.-P., Warren, J. M., Werner, C., Xia, J., Yang, B., Zak, D. R. and Norby, R. J.: Decadal biomass increment in early secondary succession woody ecosystems is increased by CO_2 enrichment, *Nat. Commun.*, 10(1), 454, doi:10.1038/s41467-019-08348-1, 2019.

Wang, Y. P., Rey, A. and Jarvis, P. G.: Carbon balance of young birch trees grown in ambient and elevated atmospheric CO_2 concentrations, *Glob. Chang. Biol.*, 4(8), 797–807, doi:10.1046/j.1365-2486.1998.00170.x, 1998.

Wujeska-Klause, A., Crous, K. Y., Ghannoum, O. and Ellsworth, D. S.: Lower photorespiration in elevated CO_2 reduces leaf N concentrations in mature *Eucalyptus* trees in the field, *Glob. Chang. Biol.*, (August 2018), 1–14, doi:10.1111/gcb.14555, 2019.

Wullschleger, S. D.: Biochemical Limitations to Carbon Assimilation in C 3 Plants—A Retrospective Analysis of the A/C_i Curves from 109 Species, *J. Exp. Bot.*, 44(5), 907–920, doi:10.1093/jxb/44.5.907, 1993.

Yang, J., Medlyn, B. E., De Kauwe, M. G. and Duursma, R. A.: Applying the concept of ecohydrological equilibrium to predict steady state leaf area index, *J. Adv. Model. Earth Syst.*, 10(8), 1740–1758, doi:10.1029/2017MS001169, 2018.

Yang J, Duursma RA, De Kauwe MG, Kumarathunge D, Jiang M, Mahmud K, Gimeno TE, Crous KY, Ellsworth DS, Peters J, Choat B, Eamus D, Medlyn BE (2019) Incorporating non-stomatal limitation improves the performance of leaf and canopy models at high vapour pressure deficit. Tree Physiol. https://academic.oup.com/treephys/advance-article/doi/10.1093/treephys/tpz103/5586169

Zaehle, S., Medlyn, B. E., De Kauwe, M. G., Walker, A. P., Dietze, M. C., Hickler, T., Luo, Y., Wang, Y. P., El-Masri, B., Thornton, P., Jain, A., Wang, S., Warlind, D., Weng, E., Parton, W., Iversen, C. M., Gallet-Budynek, A., Mccarthy, H., Finzi, A., Hanson, P. J., Prentice, I. C., Oren, R. and Norby, R. J.: Evaluation of 11 terrestrial carbon-nitrogen cycle models against observations from two temperate Free-Air CO_2 Enrichment studies, *New Phytol.*, 202(3), 803–822, doi:10.1111/nph.12697, 2014.

Zhu, Z., Piao, S., Myneni, R. B., Huang, M., Zeng, Z., Canadell, J. G., Ciais, P., Sitch, S., Friedlingstein, P., Arneth, A., Liu, R., Mao, J., Pan, Y., Peng, S., Peñuelas, J. and Poulter, B.: Greening of the Earth and its drivers, *Nat. Clim. Chang.*, 6, early online, doi:10.1038/NCLIMATE3004, 2016.

Figures and Captions

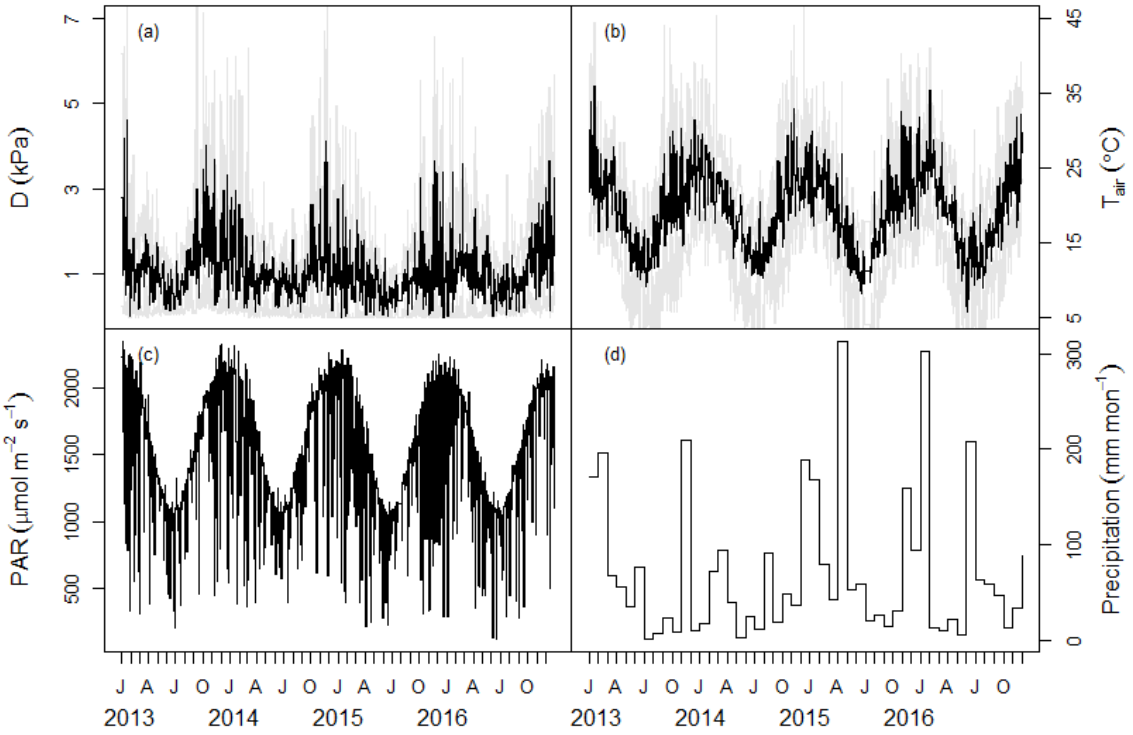

Figure 1. Meteorological data measured at the site during the period 2013-2016. Panels show (a) daily mean vapour pressure deficit (D) with shaded area marking the maximum and minimum of the day, (b) daily mean air temperature (T_{air}) with shaded area marking the maximum and minimum of the day, (c) daily maximum photosynthetically active radiation (PAR), and (d) monthly total precipitation. Note that precipitation has no direct impact in the model but modifies stomatal conductance via the change in soil moisture.

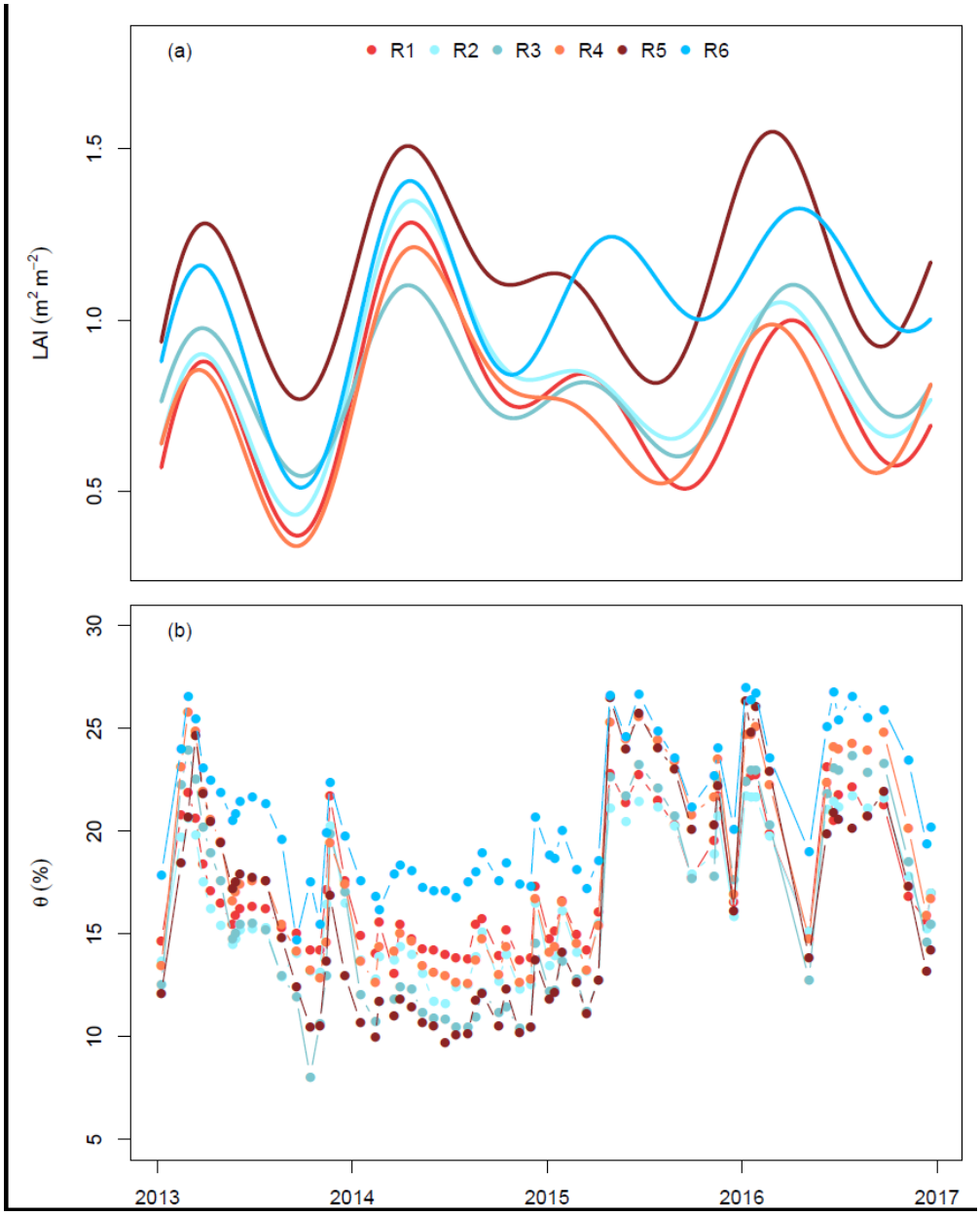

Figure 2. (a) Leaf area index (LAI) and (b) soil volumetric water content (θ) used to drive the model. LAI was estimated in each ring from measurements of understorey PAR and smoothed using a generalized additive model following Duursma et al. (2016). θ was measured using neutron probes in the top 150 cm biweekly (Gimeno et al. 2018). Each line colour indicates a different plot. Red colours show elevated CO_2 plots (treatment), while blue colours show ambient CO_2 plots (control). The x-axis ticks mark the start of each year.

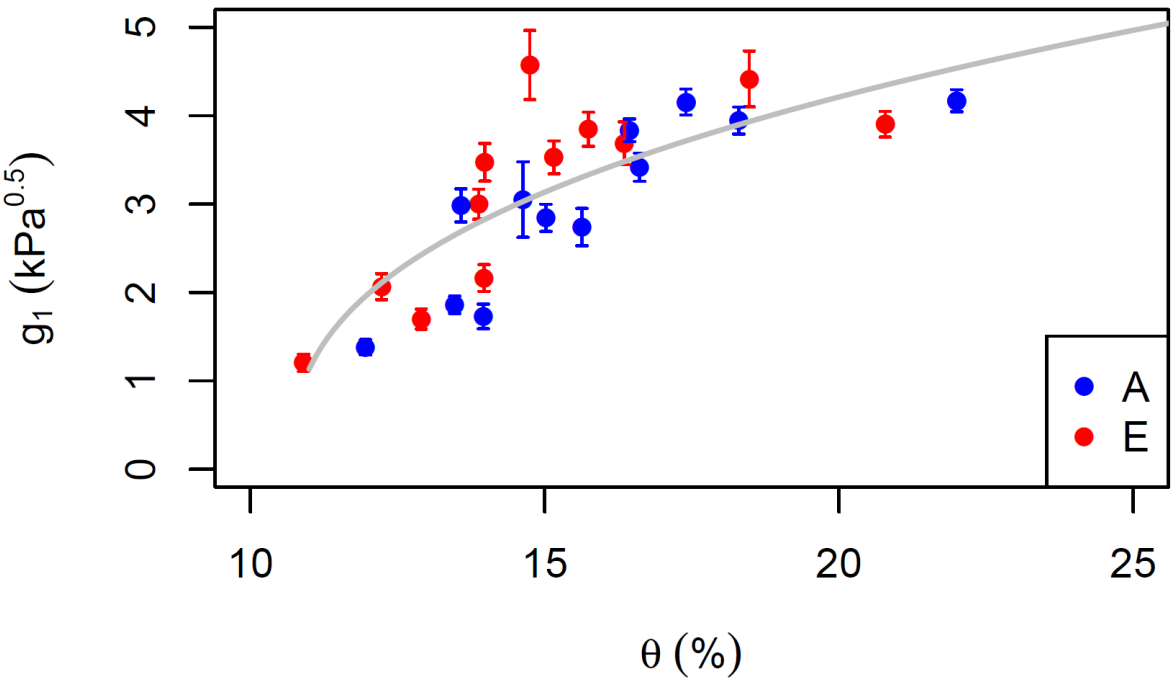

Figure 3. The impact of soil moisture content (θ) in the top 150 cm on stomatal regulation. g_1 parameter values are fitted to measurements of leaf gas exchange grouped by month and treatment. Red dots are fitted to data from elevated rings while blue are ambient rings. Error bars indicate the standard errors of the fitted values. The grey line shows the fit of Eqn. 2 to the data.

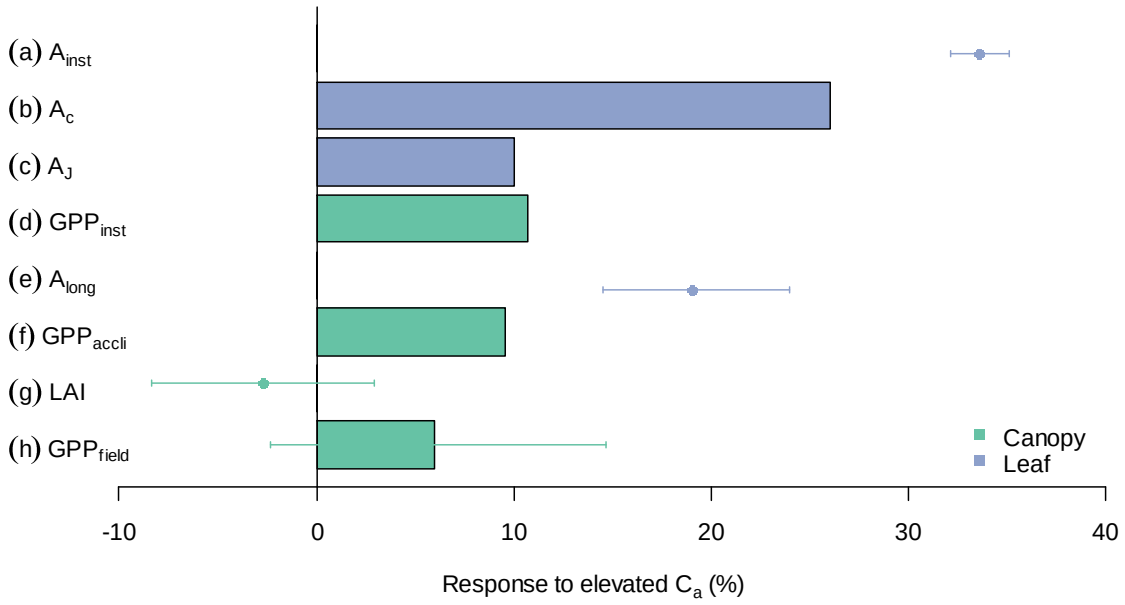

Figure 4. The response of photosynthesis to eC_a on different scales and limited by different factors. In summary, from top to bottom, the figure demonstrates how a large increase in leaf photosynthesis can diminish into a non-statistically significant change in canopy GPP under eC_a. Entries from top to bottom are as follows. (a) A_{inst}, the instantaneous response of leaf photosynthesis to eC_a obtained from A-C_i measurements in ambient rings (error bars indicate 95% CI). (b) A_c, the modelled response of Rubisco-limited leaf photosynthesis, assuming no down-regulation, averaged over the range of diurnal air temperatures experienced during the experimental period. (c) A_J, the modelled response of RuBP-regeneration limited leaf photosynthesis. (d) GPP_{inst}, the direct effect of eC_a on canopy GPP, modelled with MAESPA, assuming no downregulation of photosynthesis and averaged across all six rings. (e) A_{long}, the long-term response of leaf photosynthesis to eC_a obtained from leaf photosynthesis measured at treatment CO_2 concentrations (see Ellsworth et al. 2017). This value is different from A_{inst} because it incorporates photosynthetic acclimation. (f) GPP_{long}, the effect of eC_a on canopy GPP once the measured down-regulation of V_{cmax} is taken into account. (g) LAI, the measured difference in average LAI between eC_a and ambient C_a rings over the experiment period (data from Duursma et al. 2016). (h) GPP_{field}, the GPP response modelled with MAESPA comparing the three elevated rings with the three ambient rings. The bars represent model outputs while points represent observations. See text for further explanation.

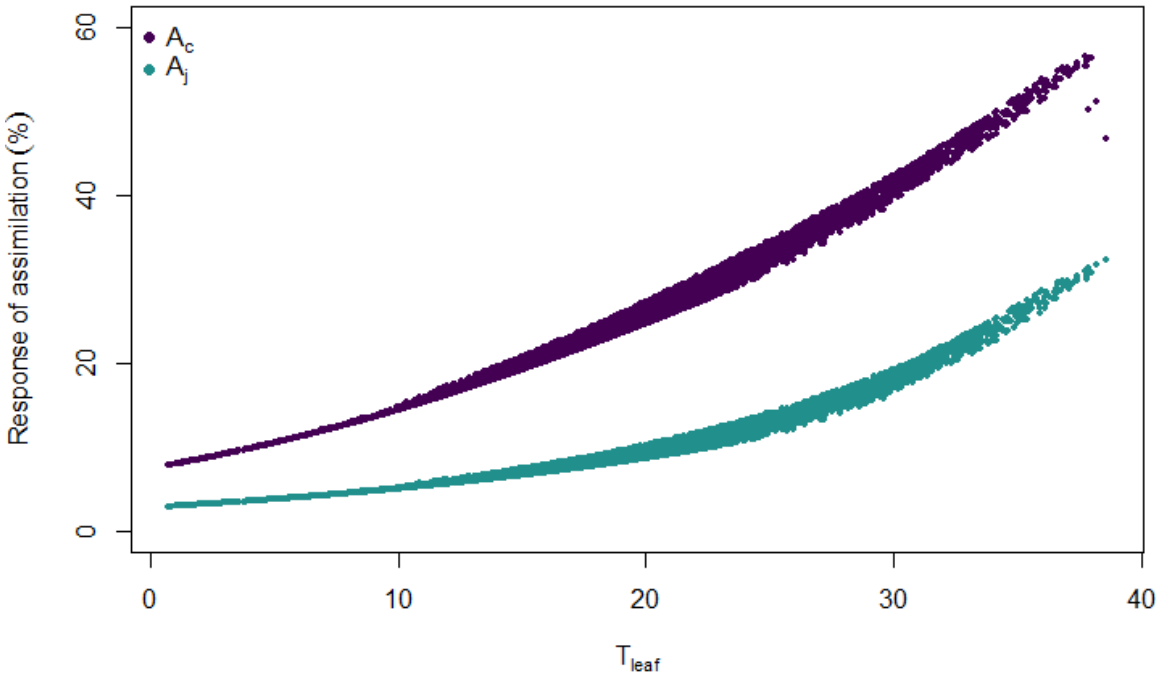

Figure 5. The modelled C_a response of Rubisco-limited leaf photosynthesis (A_c) and RuBP-regeneration-limited leaf photosynthesis (A_J) to leaf temperature (T_{leaf}). The responses are calculated for temperatures during the period 2013-2016. Parameters are as given in Table 1, except that $V_{cmax.25}$ and g_1 were assumed to be constant for clarity (g_1 = 3.3 $kPa^{0.5}$ and $V_{cmax.25}$ = 90 $\mu mol\ m^{-2}\ s^{-1}$).

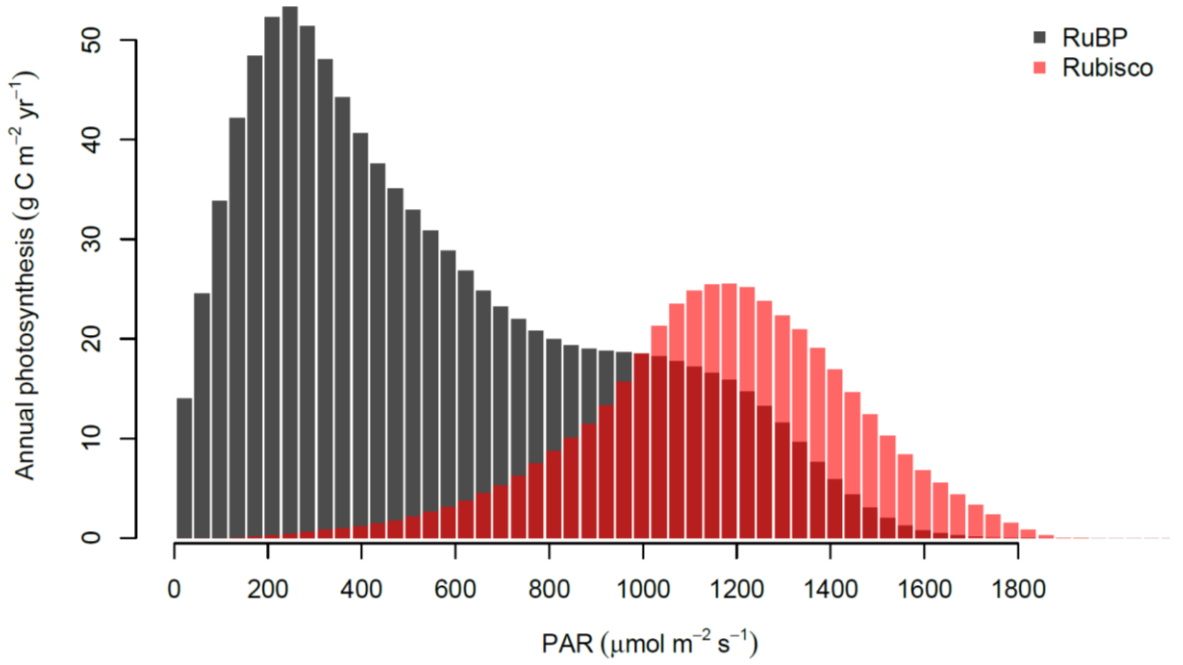

Figure 6. Distribution of average annual photosynthesis limited by Rubisco activity and RuBP-regeneration in bins of PAR (30 µmol m^{-2} s^{-1})., as calculated by MAESPA across all rings during 2013-2016. The histogram was constructed by calculating the photosynthesis (either limited by Rubisco or RuBP) falling into each bin for every half-hour in the "ambient scenario". These values were then summed to each year and ring and averaged over six rings and four years.

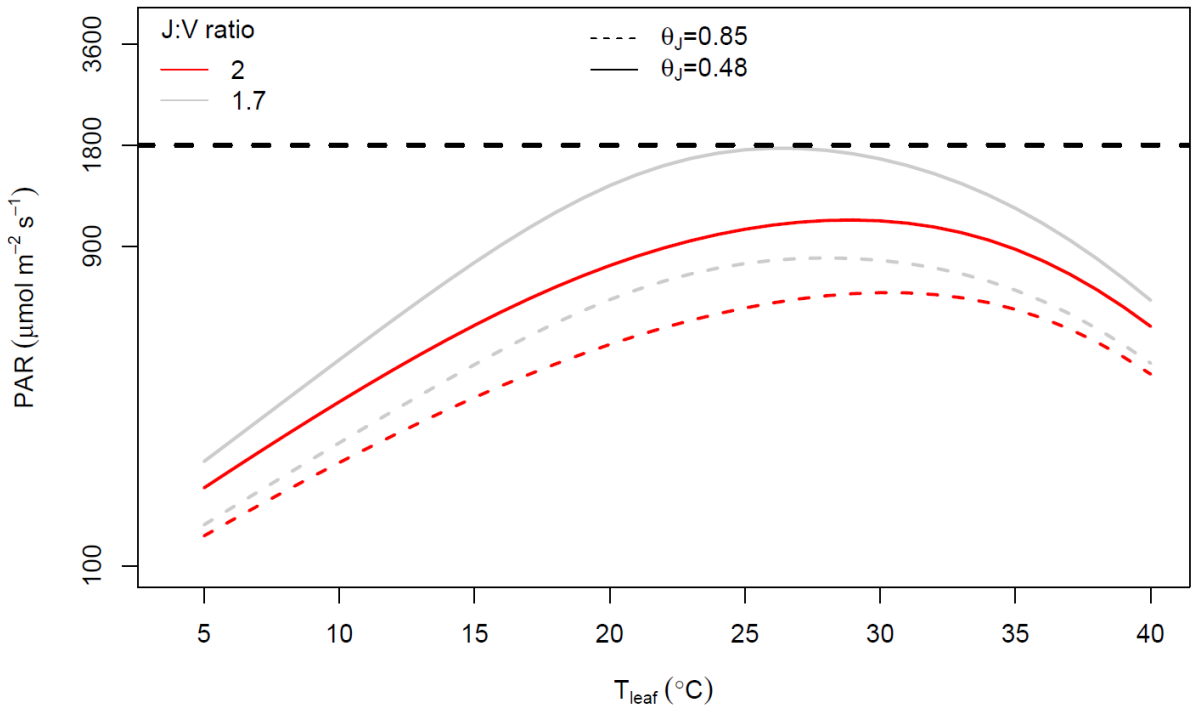

Figure 7. Estimated PAR value at which limitation to photosynthesis shifts from RuBP regeneration to Rubisco at different leaf temperatures and J:V ratios. Rubisco limitation occurs at PAR values above the curves; RuBP regeneration limitation occurs below the curves. The curves were calculated using the Photosyn *function in the*

plantecophys *R package (Duursma, 2015). The parameters other than PAR and* T_{leaf} *were assumed to be constant:* C_a *= 390 µmol mol*$^{-1}$*;* D *=1.5 kPa;* g_1 *= 3.3 kPa*$^{0.5}$*;* $V_{cmax.25}$ *= 90 µmol m*$^{-2}$ *s*$^{-1}$*. The temperature and light dependences of photosynthesis were assumed to be the same as in MAESPA. The grey line was predicted by assuming* $J_{max.25}$ *= 153 µmol m*$^{-2}$ *s*$^{-1}$ *(i.e., J:V ratio= 1.7). This J:V ratio was observed consistently in EucFACE across campaigns and rings. The red line was predicted by assuming* $J_{max.25}$ *= 180 µmol m*$^{-2}$ *s*$^{-1}$ *(i.e., J:V ratio= 2). This J:V ratio was commonly reported and used in other studies. The horizontal dashed line shows the PAR = 1800 µmol m*$^{-2}$ *s*$^{-1}$ *at which leaf-level measurements of EucFACE were made. Note the log scale of the y axis. The dashed curves are based on quantum yield of electron transport (*α_J*; mol mol*$^{-1}$*) and convexity of light response of RuBP;* θ_J *; unitless)values from CABLE model (Haverd et al., 2018).*

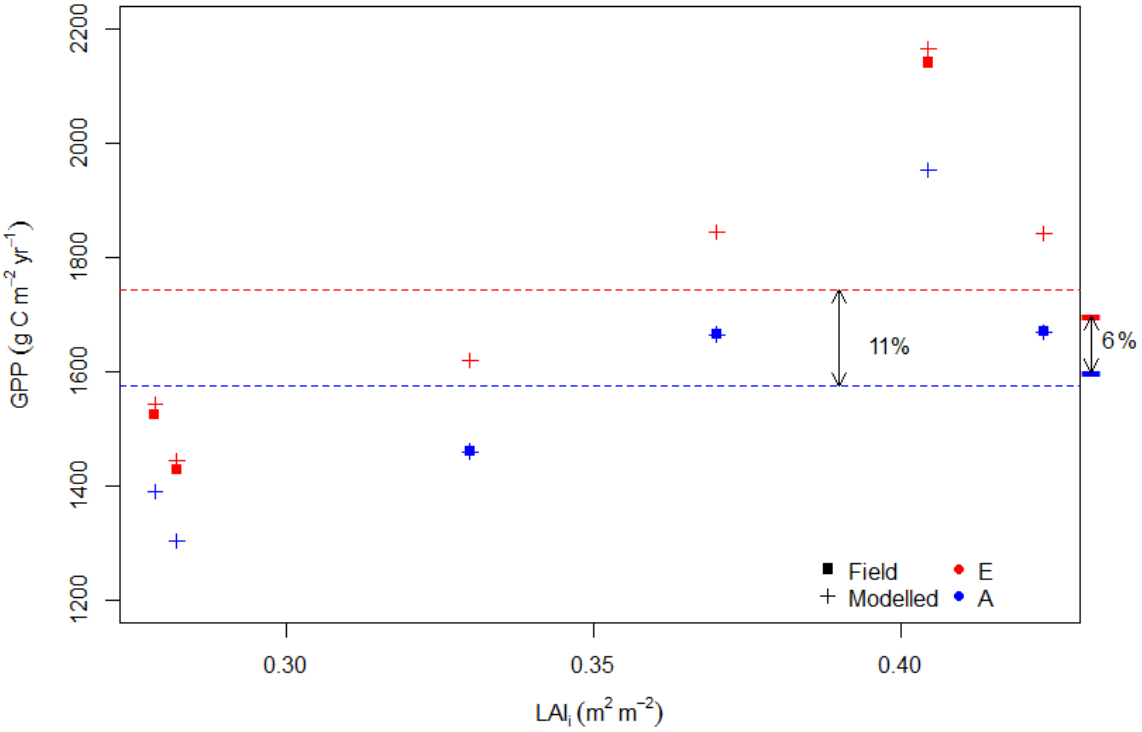

Figure 8. The four-year average GPP of all six rings under ambient and eC_a *plotted against initial leaf area index (*LAI_i*).* LAI_i *is the LAI measurement taken on the 26 October 2012 and is a proxy for the inherent variation among the rings. For all six rings, estimated GPP is shown for ambient* C_a *(blue) and* eC_a *(red). Crosses indicate GPP from simulations by varying* C_a *and squares indicate GPP as under field conditions. The flat bars on the right hand-side of the plot indicate the average ambient* C_a *GPP for ambient rings only (the average of blue squares) and average* eC_a *GPP for elevated rings only (the average of red squares). Dashed lines indicate average ambient* C_a *(the average of blue crosses) and* eC_a *GPP across all six rings (the average of red crosses). The flat bars thus mark the modelled response without inter-ring variability while the dashed lines mark the modelled realized response, including inter-ring variability.*